Mathematical model of SIR epidemic system (COVID-19) with fractional derivative: stability and numerical analysis

Check for updates

Rubayyi T. Alqahtani[1*]

*Correspondence:
rtalqahtani@imamu.edu.sa
[1] Department of Mathematics and
Statistics, College of Science, Imam
Mohammad Ibn Saud Islamic
University (IMSIU), Riyadh, Saudi
Arabia

Abstract

In this paper, we study and analyze the susceptible-infectious-removed (SIR) dynamics considering the effect of health system. We consider a general incidence rate function and the recovery rate as functions of the number of hospital beds. We prove the existence, uniqueness, and boundedness of the model. We investigate all possible steady-state solutions of the model and their stability. The analysis shows that the free steady state is locally stable when the basic reproduction number R_0 is less than unity and unstable when $R_0 > 1$. The analysis shows that the phenomenon of backward bifurcation occurs when $R_0 < 1$. Then we investigate the model using the concept of fractional differential operator. Finally, we perform numerical simulations to illustrate the theoretical analysis and study the effect of the parameters on the model for various fractional orders.

Keywords: SIR model; Stability; Nonlinear recovery rate; Hospital bed; Backward bifurcation; Fractional model

1 Introduction

The spread of Covid-19 diseases is a very complex phenomenon carried out by many researchers. Many mathematical models were proposed including complex and simple mathematical models to understand the disease behavior. Faal et al. [1] proposed a model for the spread of the COVID-19 disease taking into account the superspreader, hospitalized, and fatality class. The authors analyzed the local stability of the steady-state solution and the model sensitivity. Mandal et al. [2] introduced a mathematical model taking into account a quarantine class and governmental intervention measures. In this study, the authors consider the basic reproduction number as an important parameter in analyzing the dynamics of the model. Recently, significant works were carried out to study the behavior of COVID-19 by means of mathematical models. Lin et al. [3] proposed SEIR models for the COVID-19 using data from China considering the impact of social isolation policies including governmental actions. The model successfully captures the course of the COVID-19 outbreak, whereas Wells et al. [4] and Gostic et al. [5] consider the impact of travel restrictions and border control on the global spread of the COVID-19.

Springer

The SIR model is commonly used for disease modeling, in particular, for the COVID-19 analysis [6–8]. The dynamic behavior of SIR model, including the stability, bifurcation, and chaos, has been studied over many decades [9–12]. In most studies the authors assume that the recovery rate is a constant. However, in reality the recovery rate depends on time of recovering process such as the health system, including the number of hospital beds and medicines.

In recent years, many researchers have studied the systems of differential equations with fractional operators [13–15]. The epidemic models involving a fractional operator were also investigated by many authors because they deeply show biological and physical perspectives of the diseases [16, 17].

Rao et al. [18] studied an SIRS epidemic model assuming different death rates for each subclass, and the fraction of newborn children is represented by the parameter p. In this paper, we propose and analyze the extended SIRS epidemic model presented in [18] with the concept of fractional differential operator. In fact, we propose and study a model including three nonlinear differential equations with general incidence rate function and nonlinear recovery rate depending on the health system. The main focus of this study is analyzing the basic properties of model and demonstrating the stability properties of the model.

The rest of the paper is arranged as follows. We propose a dynamical model in Sect. 2. Then we formulate and establish the existence, uniqueness, positivity, and boundedness of solutions in Sect. 3. The steady-state solutions of the model and their stability are studied in Sects. 4 and 5, whereas numerical simulations of the steady-state solution brunches has is presented in Sect. 6. Section (7) contains a detailed dynamic behavior of the model with fractional derivative. We finish this study with conclusion in Sect. 8.

2 The dimensional model

In this section, we extend the model suggested in [18] to include a nonlinear incidence rate and recovery rate. The recovery rate is a function of both the hospital bed-population ratio $b_1 > 0$ and the infected I. Thus the recovery rate α is given by [19]

$$\alpha = \alpha_0 + \frac{(\alpha_1 - \alpha_0)b_1}{I + b_1}, \tag{1}$$

where the parameter α_1 and α_0 are the maximum and minimum per capita recovery rates, respectively. The nonlinear incidence rate is generalized by the function

$$f(S, I) = \frac{\beta_1 SI}{a_1 + a_2 S + a_3 I}. \tag{2}$$

Thus the system of differential equations is given by

$$\frac{dS}{dt} = (1 - p)b - \mu_1 S - f(S, I) + \gamma R, \tag{3}$$

$$\frac{dI}{dt} = f(S, I) - (\mu_2 + \alpha)I, \tag{4}$$

$$\frac{dR}{dt} = pb - (\mu_3 + \gamma)R + \alpha I, \tag{5}$$

where the total population is split into three parts: $S(t)$ is the susceptible population, $I(t)$ is the infected population, and $R(t)$ is the recovered population, so that $N = S + I + R$. The details and interpretation of the model can be found in [18]. We assume that all parameters are positive.

3　Basic properties of model
3.1　Positivity of solution
In this section, we prove that under nonnegative conditions, the model solutions are positive.

Theorem 1 *Let $S_0, I_0, R_0 \geq 0$. The solution of* (3)–(5) *with* $(S(0), I(0), R(0)) = (S_0, I_0, R_0)$ *is nonnegative, that is,* $S(t), I(t), R(t) \geq 0$ *for* $t > 0$.

Proof Let $x(t) = (S(t), I(t), R(t))$ be the solution of system under initial conditions $x_0 = (S(0), I(0), R(0)) = (S_0, I_0, R_0) \geq 0$.

By the continuity of solution, for all of $S(t), I(t), R(t)$ that have positive initial values at $t = 0$, we have the existence of an interval $(0, t_0)$ such that $S(t), I(t), R(t) \geq 0$ for $0 < t < t_0$. We will prove that $t_0 = \infty$.

If $S(t_1) = 0$ for $t_1 \geq 0$ and other solutions stay positive at $t = t_1$, then

$$\frac{dS}{dt}(t = t_1) = (1 - p)A + \gamma R > 0. \tag{6}$$

This ensures that at any time the solution reaches the axis, its derivative increases, and the function $S(t)$ does not cross to negative part. We can show by similar analysis that

$$\frac{dI}{dt}(t = t_1) = 0, \tag{7}$$

$$\frac{dR}{dt}(t = t_1) = pb + \alpha I \geq 0. \tag{8}$$

So $x(t)$ never crosses the axes $S = 0, I = 0, R = 0$ when it touches them. Thus, for any positive initial conditions, all equation solutions are positive. □

Theorem 1 *Let* $(S(t), I(t), R(t))$ *be the solution of system* (3)–(5) *with initial conditions* (S_0, I_0, R_0), *and let* $\mu = \min(\mu_1, \mu_2, \mu_3)$. *The compact set*

$$\Psi = \left\{ (S(t), I(t), R(t)) \in \mathbb{R}_+^3, W \leq b/\mu \right\} \tag{9}$$

is positively invariant and attracts all solutions in $\mathbb{R}_+^3$.

Proof Let $W(t) = S(t) + I(t) + R(t)$. Then from the system (3)–(5) we have

$$\frac{dW}{dt} \leq b - \min(\mu_1, \mu_2, \mu_3)W = b - \mu W.$$

This implies that

$$\frac{dW}{dt} + \mu W \leq b. \tag{10}$$

Solving (10), we obtain

$$0 < W \leq \frac{b}{\mu} + \left(W(0) - \frac{b}{\mu} \right) \exp(-\mu t), \tag{11}$$

where $W(0)$ is the initial condition. Thus $0 < W(t) < \frac{b}{\mu}$ as t reaches infinity, and hence Ψ is a positively invariant and attractive set. □

3.2 Basic reproduction number

We use the next-generation matrix method [24] to calculate the reproduction number R_0 of model (3)–(5):

$$R_0 = \frac{(\gamma_1 + \mu_3[1-p])b\beta_1}{a_2(\gamma 1 + \mu_3[1-p])(\alpha_1 + \mu_2)b + a_1\mu_1(\mu_3 + \gamma_1)(\alpha_1 + \mu_2)}. \tag{12}$$

4 Equilibria

In this section, we consider the number of equilibrium solutions of model (3)–(5). It is clear that the model has a disease-free equilibrium given by

$$E_0(S, I, R) = \left(\frac{b(\gamma_1 + \mu_3[1-p])}{\mu_1(\mu_3 + \gamma_1)}, 0, \frac{pb}{\mu_3 + \gamma_1} \right). \tag{13}$$

The non-free steady state of model (3)–(5) can be obtained by setting the right sides to zero. From equations (3)–(5) we have

$$S = \frac{(\alpha_0 + \mu_2)I^2 + ((p-1)b + b_1[\alpha_1 + \mu_2] - \gamma_1 R)I + bb_1(p-1) - \gamma_1 b_1 R}{\mu_1(I + b_1)}, \tag{14}$$

$$R = \frac{\alpha_0 I^2 + (b_1\alpha_1 + pb)I + bb_1 p}{(I + b_1)(\mu_3 + \gamma_1)}. \tag{15}$$

Substituting equations ((14) and (15)) into equation (3), we obtain

$$E_1(I) = c_3 I^3 + c_2 I^2 + c_1 I + c_0 = 0, \tag{16}$$

where c_0, c_1, c_2, and c_3 are defined by

$$c_3 = \left((\alpha_0 + \mu_2)\mu_3 + \gamma_1\mu_2\right)\beta_1 + (\alpha_0 + \mu_2)(a_2\alpha_0 + a_2\mu_2 - a_3\mu_1)\mu_3 \tag{17}$$
$$\quad + \gamma_1(\alpha_0 + \mu_2)(a_2\mu_2 - a_3\mu_1),$$

$$c_2 = -\left(\gamma_1 + \mu_3(1-p)\right)(a_2\alpha_0 + a_2\mu_2 - \beta_1)b + (c_{21} + c_{22} + c_{23})b_1 + c_{24},$$

$$c_1 = -\left(\gamma_1 + \mu_3(1-p)\right)\left(a_2[\alpha_0 + \alpha_1 + 2\mu_2] - 2\beta_1\right)b_1 b + (c_{11} + c_{12})b_1^2 + c_{13},$$

$$c_0 = b_1^2[R_0 - 1],$$

$$c_{21} = \left((2\gamma_1 + 2\mu_3)\mu_2^2 + (\gamma_1 + 2\mu_3)(\alpha_0 + \alpha_1)\mu_2 + 2\alpha_0\alpha_1\mu_3\right)a_2,$$

$$c_{22} = -\left(2\mu_1\mu_2(\mu_3 + \gamma_1) + \mu_1(\mu_3 + \gamma_1)(\alpha_0 + \alpha_1)\right)a_3,$$

$$c_{23} = -\left(2\mu_2(\gamma_1 + \mu_3) + \mu_3(\alpha_0 + \alpha_1)\right)\beta_1,$$

$$c_{24} = -a_1\mu_1(\mu_3 + \gamma_1)(\alpha_0 + \mu_2),$$

Table 1 Number of possible positive real roots of equation (16). c_4 = basic reproduction number R_0, c_5 = sign change number, c_6 = possible number of positive real roots

Case	c_3	c_2	c_1	c_0	c_4	c_5	c_6
1	−	+	+	+	$R_0 > 1$	1	1
2	−	+	+	−	$R_0 < 1$	2	0, 2
3	−	+	−	+	$R_0 > 1$	3	1, 3
4	−	+	−	−	$R_0 < 1$	2	0, 2
5	−	−	+	+	$R_0 > 1$	1	1
6	−	−	+	−	$R_0 < 1$	2	0, 2
7	−	−	−	+	$R_0 > 1$	1	1
8	−	−	−	−	$R_0 < 1$	0	0

$$c_{11} = (\alpha_1 + \mu_2)(\mu_3\alpha_1 + \gamma_1\mu_2 + \mu_2\mu_3)a_2,$$

$$c_{12} = -\big[(\mu_3 + \gamma_1)(\alpha_1 + \mu_2)\mu_1 a_3 + (\mu_3\alpha_1 + \gamma_1\mu_2 + \mu_2\mu_3)\beta_1\big],$$

$$c_{13} = -(\mu_3 + \gamma_1)(\alpha_0 + \alpha_1 + 2\mu_2)b_1 a_1 \mu_1.$$

If $R_0 = 1$, then $c_0 = 0$, so equation (16) reduces to the equation

$$E_1(I) = I\big[a_3 I^2 + a_2 I + a_1\big] = 0, \tag{18}$$

where $I = 0$ is the disease-free equilibrium. By equation (16) the coefficient $c_0 > 0$ when $R_0 > 1$ and $c_0 < 0$ when $R_0 < 1$. Thus the number of possible positive real roots depends on the values of c_3, c_2, and c_1. The possible roots analyzed by the Descartes rule of signs are shown in Table 1.

Theorem 2 *System* (3)–(5):

1. *has a one equilibrium if the basic reproduction number is greater than* 1 *and Cases* 1, 5, *and* 7 *are satisfied*;
2. *can have more than one equilibrium if the basic reproduction number is greater than* 1 *and Case* 3 *is satisfied*;
3. *can have two or more equilibria if the basic reproduction number is less than* 1 *and Cases* 2, 4, *and* 6 *are satisfied*.

The existence of multiple steady state suggests the possibility of backward bifurcation where the phenomenon of three branches of steady-state equilibrium occurs at the same point.

5 Stability

In this section, we focus on analysis of the stability of the equilibrium of equations (3)–(5). We study the stabilities of two types of the disease equilibrium, that is, E_0 and E_1.

5.1 Local stability of the disease-free equilibrium

In this section, we study the stability of the free equilibrium E_0. The Jacobian matrix of system (3)–(5) at E_0 is

$$J(E_0) = \begin{bmatrix} -\mu & j_{12} & \gamma_1 \\ 0 & j_{22} & 0 \\ 0 & \alpha_1 & -[\mu_3 + \gamma_1] \end{bmatrix}, \tag{19}$$

where

$$J_{12} = -\frac{\beta_1 b(\gamma_1 + \mu 3_1[1-p])}{\mu_1(\mu_3 + \gamma_1)}\left(\frac{a_2 b(\gamma_1 + \mu_3[1-p])}{\mu_1(\mu_3 + \gamma_1)} + a_1\right)^{-1} < 0,$$

$$J_{22} = -\frac{(\gamma_1 + \mu_3[1-p])(a_2\alpha_1 + a_2\mu_2 - \beta_1)b + a_1\mu 1(\mu_3 + \gamma_1)(\alpha_1 + \mu_2)}{a_2 b(\gamma_1 + \mu_3[1-p]) + a_1\mu_1(\mu_3 + \gamma_1)}.$$

The eigenvalues of matrix (19) are given by

$$\lambda_i = \begin{bmatrix} -\mu_1 \\ -[\mu_3 + \gamma_1] \\ J_{22} \end{bmatrix}. \tag{20}$$

A simple calculation shows that $J_{22} = R_0 - 1$. So, we have the following result.

Lemma 1 *The free steady-state solution E_0 is locally asymptotically stable if $R_0 < 1$ and is unstable if $R_0 > 1$.*

5.2 Stability of equilibria E_1

In this section, we show that the nonfree steady-state solution E_1 of system (3)–(5) is stable under specific condition. The Jacobian of the system can be written as

$$J(E_1) = \begin{bmatrix} -J_{11} & -J_{12} & \gamma_1 \\ J_{21} & -J_{22} & 0 \\ 0 & J_{32} & -[\mu_3 + \gamma_1] \end{bmatrix}, \tag{21}$$

where

$$J_{11} = \left[\frac{\beta_1 I(Ia_3 + a_1)}{(Ia_3 + a_2 S + a_1)^2} + \mu_1\right], \tag{22}$$

$$J_{12} = \left[\frac{\beta_1 S(a_2 S + a_1)}{(Ia_3 + a_2 S + a_1)^2}\right],$$

$$J_{21} = \frac{\beta_1 I(Ia_3 + a_1)}{(Ia_3 + a_2 S + a_1)^2},$$

$$J_{22} = \frac{(\alpha_1 - \alpha_0)b_1^2}{(I + b_1)^2} + \alpha_0 - \frac{\beta_1 S(a_2 S + a_1)}{(Ia_3 + a_2 S + a_1)^2} + \mu_2,$$

$$J_{32} = \frac{(\alpha_1 - \alpha_0)b_1^2}{(I + b_1)^2} + \alpha_0. \tag{23}$$

From equation (4) we get the following relations:

$$\frac{\beta_1 SI}{a_1 + a_2 S + a_3 I} - \left(\mu_2 + \alpha_0 + \frac{(\alpha_1 - \alpha_0)b_1}{I + b_1}\right)I = 0, \tag{24}$$

$$J_{22} = -\frac{\beta_1 SIa_3}{(Ia_3 + a_2 S + a_1)^2} + \frac{(\alpha_1 - \alpha_0)b_1 I}{(I + b_1)^2}. \tag{25}$$

By simple analysis we get that the characteristics equation of $J(E_1)$ is

$$\lambda^3 + B_1\lambda^2 + B_2\lambda + B_3, \tag{26}$$

where

$$B_1 = J_{22} + J_{11} + \mu_1 + \mu_3 + \gamma_1,$$

$$B_2 = (J_{12} + J_{22} + \gamma_1 + \mu_3)J_{11} + (J_{22} + \gamma_1 + \mu_3)\mu_1 + (\gamma_1 + \mu_3)J_{22},$$

$$B_3 = \big((J_{12} + J_{22} - J_{32})\gamma_1 + \mu_3(J_{12} + J_{22})\big)J_{11} + J_{22}\mu_1[\gamma_1 + \mu_3].$$

We further use the Rough–Hurtwiz criterion to show the stability of the steady state E_1. We have

$$B_1B_2 - B_3 = B_{11}J_{11}{}^2 + B_{22}J_{11} + B_{33},$$

$$B_{11} = (J_{22} + J_{12} + \mu_3 + \gamma_1),$$

$$B_{22} = \big(J_{22}{}^2 + \big(J_{12} + 2[\mu_3 + \mu_1 + \gamma_1]\big)J_{22} + \gamma_1{}^2 + \big(J_{32} + 2[\mu_3 + \mu_1]\big)\gamma_1 \tag{27}$$
$$\qquad + \mu_1[J_{12} + 2\mu_3] + \mu_3{}^2\big),$$

$$B_{33} = (\mu_3 + \mu_1 + \gamma_1)J_{22}{}^2 + (\mu_3 + \mu_1 + \gamma_1)^2 J_{22} + \mu_1(\mu_3 + \mu_1 + \gamma_1)(\mu_3 + \gamma_1).$$

By the Routh–Hurwitz theorem E_1 is locally asymptotically stable when $B_1 > 0$, $B_3 > 0$, and $B_1B_2 - B_3 > 0$. Theses conditions are satisfied when the following condition holds:

$$\frac{S}{(Ia_3 + a_2S + a_1)^2} < \frac{\mu_2}{\beta_1}. \tag{28}$$

Thus we have following results.

Lemma 2 *The steady-state solution E_1 of model* (3)–(5) *is locally asymptotically if*

$$\frac{S}{(Ia_3 + a_2S + a_1)^2} < \frac{\mu_2}{\beta_1}. \tag{29}$$

Theorem 3 *The backward bifurcation occurs if $b_1 < b_{cr}$, and no backward bifurcation otherwise.*

Proof We show the conditions for the existence of backward bifurcation for system (3)–(5) using the center manifold approach.

First, making a transformation of variables, we have $x_1 = S, x_2 = I, x_3 = R$. Then model (3)–(5) can be written in the form $\frac{dX}{dt} = F(X)$, where $F = (f_1, f_2, f_3)$. Hence

$$\frac{dS}{dt} = f_1 = (1-p)b - \mu_1 S - f(S,I) + \gamma R, \tag{30}$$

$$\frac{dI}{dt} = f_2 = f(S) - (\mu_2 + \alpha)I, \tag{31}$$

$$\frac{dR}{dt} = f_3 = pb - (\mu_3 + \gamma)R + \alpha I, \tag{32}$$

$$\alpha = \alpha_0 + \frac{(\alpha_1 - \alpha_0)b_1}{I + b_1},$$

$$f(S,I) = \frac{\beta_1 SI}{a_1 + a_2 S + a_3 I}.$$

Now let $\beta_1 = \beta_1^*$ be the bifurcation parameter. When $R_0 = 1$, we have the following relation:

$$\beta_1 = \frac{S_0 a_2[\alpha_1 + \mu_2] + a_1[\alpha_1 + \mu_2]}{S_0}, \tag{33}$$

and the model equation has one zero eigenvalue, and the other eigenvalues are negative. The behavior of the system near $\beta_1 = \beta_1^*$ can be studied by applied the center manifold theory. The Jacobian matrix at free steady state E_0 is

$$J(E_0) = \begin{bmatrix} -\mu_1 & -\frac{\beta_1 S_0}{S_0 a_2 + a_1} & \gamma_1 \\ 0 & \frac{\beta_1 S_0}{S_0 a_2 + a_1} - \alpha_1 - \mu_2 & 0 \\ 0 & \alpha_1 & -[\mu_3 + \gamma_1] \end{bmatrix}. \tag{34}$$

The right eigenvectors can be obtained as $W = (w_1, w_2, w_3)^T$, where $(w_1, w_2, w_3)^T = (-\frac{\alpha_1 \mu_3 + \mu_2[\gamma_1 + \mu_3]}{\alpha_1 \mu_1}, \frac{\mu_3 + \gamma_1}{\alpha_1}, 1)$. The left eigenvectors can be obtained as $V = (v_1, v_2, v_3) = (0, 1, 0)$. The existence of backward bifurcation depends on the coefficients **a** and **b** in [25, Theorem 4.1]. The nonzero partial derivatives of system (30)–(32) at disease-free equilibrium E_0 are

$$\frac{\partial f_1}{\partial x_1 \partial x_2}(E_0) = -\frac{(\alpha_1 + \mu_2) a_1}{S_0(a_2 S_0 + a_1)}, \tag{35}$$

$$\frac{\partial f_1}{\partial x_2 \partial x_1}(E_0) = -\frac{(\alpha_1 + \mu_2) a_1}{S_0(a_2 S_0 + a_1)}, \tag{36}$$

$$\frac{\partial f_1}{\partial x_2 \partial x_2}(E_0) = \frac{2a_3(\alpha_1 + \mu_2)}{a_2 S_0 + a_1}, \tag{37}$$

$$\frac{\partial f_2}{\partial x_1 \partial x_2}(E_0) = \frac{(\alpha_1 + \mu_2) a_1}{S_0(a_2 S_0 + a_1)}, \tag{38}$$

$$\frac{\partial f_2}{\partial x_2 \partial x_1}(E_0) = \frac{(\alpha_1 + \mu_2) a_1}{S_0(a_2 S_0 + a_1)}, \tag{39}$$

$$\frac{\partial f_2}{\partial x_2 \partial x_2}(E_0) = -2\left(\frac{(\alpha_1 + \mu_2) a_3}{a_2 S_0 + a_1} + \frac{\alpha_0 - \alpha_1}{b_1}\right), \tag{40}$$

$$\frac{\partial f_3}{\partial x_2 \partial x_2}(E_0) = 2\left(\frac{\alpha_0 - \alpha_1}{b_1}\right). \tag{41}$$

The coefficient **a** is obtained as

$$\mathbf{a} = \sum_{k,i,j=1}^{3} v_k w_i w_j \frac{\partial f_k}{\partial x_i \partial x_j} = w_1 w_2 \frac{\partial f_2}{\partial x_1 \partial x_2}(E_0) + w_2 w_1 \frac{\partial f_2}{\partial x_2 \partial x_1}(E_0) + w_2 w_2 \frac{\partial f_2}{\partial x_2 \partial x_2}(E_0)$$

$$= -2\left(\frac{a_3(\mu_3 + \gamma_1)^2(\alpha_1 + \mu_2)}{\alpha_1^2(a_2 S_0 + a_1)} + \frac{(\alpha_0 - \alpha_1)(\mu_3 + \gamma_1)^2}{b_1 \alpha_1^2}\right)$$

$$- \frac{2(\alpha_1 \mu_3 + \mu_2[\gamma_1 + \mu_3])(\mu_3 + \gamma_1)(\alpha_1 + \mu_2) a_1}{\alpha_1^2 \mu_1 S_0(a_2 S_0 + a_1)}. \tag{42}$$

The bifurcation parameter **b** at E_0 is given by

$$\frac{\partial f_2}{\partial x_2 \partial \beta_1^*}(E_0) = \frac{S_0}{S_0 a_2 + a_1}$$

and can be obtained as

$$
\mathbf{b} = \sum_{k,i=1}^{3} v_k w_i \frac{\partial f_k}{\partial x_i \, \partial \beta_1^*} = v_2 w_2 \frac{\partial f_2}{\partial x_2 \, \partial \beta_1^*}(E_0)
$$

$$
= \frac{(\mu_3 + \gamma_1) S_0}{\alpha_1 (S_0 a_2 + a_1)} > 0. \tag{43}
$$

Clearly, **b** is always positive. According to [25, Theorem 4.1], the backward bifurcation phenomenon exists when the coefficient **a** is positive. Thus the condition for backward bifurcation is given by

$$
b_1 < b_{1,\mathrm{cr}} = \frac{\mu_1 S_0 [a_2(\mu_3 + \gamma_1)(\alpha_1 - \alpha_0)S_0 + a_1(\mu_3 + \gamma_1)(\alpha_1 - \alpha_0)]}{[\alpha_1 + \mu_2][S_0 a_3 \mu_1(\mu_3 + \gamma_1) + a_1(\alpha_1 \mu_3 + \mu_2[\gamma_1 + \mu_3])]}. \tag{44}
$$

$\square$

The existence of the backward bifurcation at $R_0 = 1$ requires condition (44) to be satisfied. When the number of hospital beds b_1 is below the critical point $b_{1,\mathrm{cr}}$, the number of hospital beds open to the public is below demand, and as a result, some patients fail to access to healthcare. In this situation, there remains a high infection leading to a backward bifurcation.
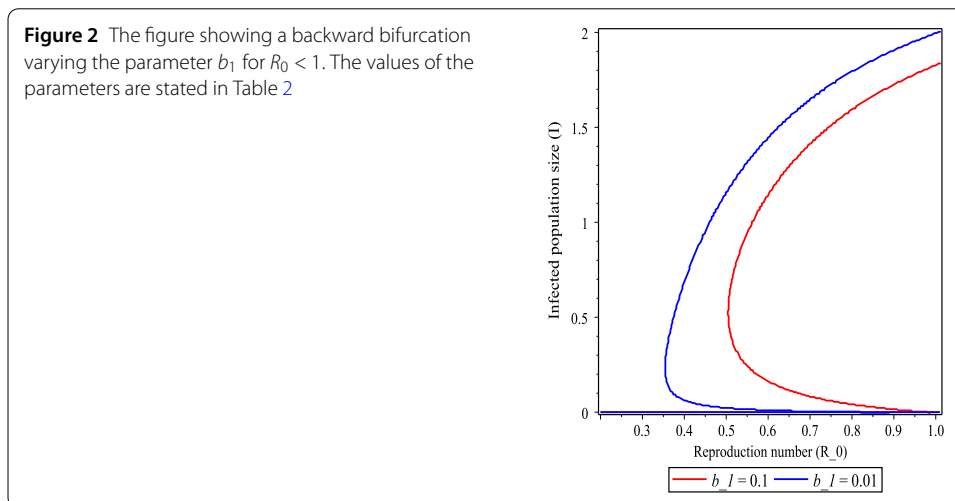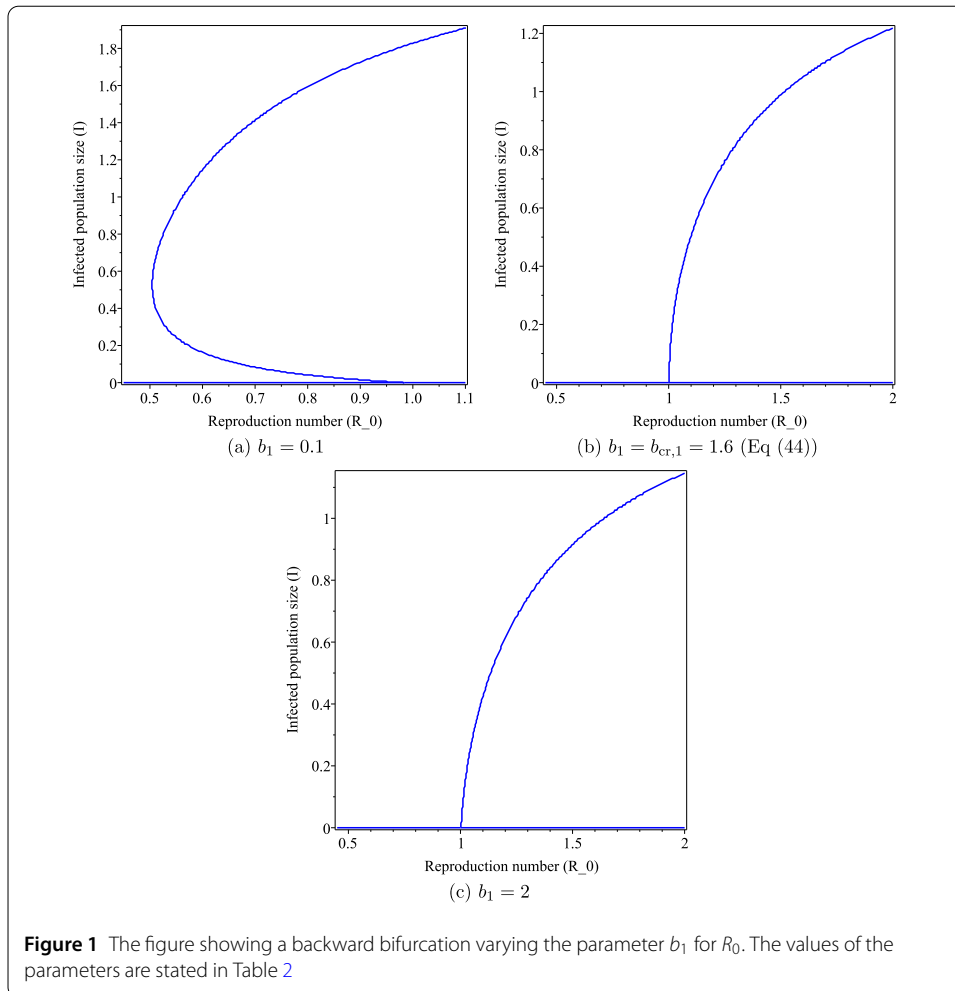
6 Numerical simulations

In this section, we carry out some numerical calculations to support our theoretical results. The values of parameters used for numerical simulations are indicated in Table 2. We study the branch of steady state with respect to the model parameters. Figure 1 shows the curves of the infected population I for different values of b_1, donated by the number of hospital beds and a specific value of general incidence rate ($a_1 = a_2 = a_3 = 1$). It shows that there is a forward bifurcation at $R_0 = 1$.

If we decrease the value of b_1 from 2 to 1.6, then the backward bifurcation does not occur. These values are higher than the critical value of $b_{1,\mathrm{cr}} = 1.64$. If we decrease the value of b_1 to 0.1, less than the critical value $b_{1,\mathrm{cr}} = 1.64$, then we can observe from Fig. 1(a) that the backward bifurcation occurs. Note that in Fig. 1(a) the above line of the curve is a stable state and the below line of the curve is an unstable state. This result indicates that

Table 2 Parameters values

Parameters	Values	Reference
b	1	[20]
p	0.8 [0,1]	[21]
α_0	0.0714	Assumed.
α_1	0.0857	Assumed.
β_1	0.5	[20]
γ	0.25	[20]
μ_1	0.2	[22]
μ_2	0.2	[22]
μ_3	0.2	[22]
b_1	[0,20] 1.9	[23]
a_1	1	Assumed.
a_2	1	Assumed.
a_3	1	Assumed.

Figure 1 The figure showing a backward bifurcation varying the parameter b_1 for R_0. The values of the parameters are stated in Table 2

Figure 2 The figure showing a backward bifurcation varying the parameter b_1 for $R_0 < 1$. The values of the parameters are stated in Table 2

in managing an infectious disease the number of hospital beds plays a significant role. Figure 2 shows the effect of the value of b_1 on the curve when the backward bifurcation occurs. We observe that as the value of b_1 decreases, the area of the curve increases.

Figure 2 shows the infected population size I as a function of reproduction number R_0 when the parameter b_1 is varied for the case $R_0 < 1$. It illustrates that as the value of b_1 increases, the infected population size I decreases. It also shows the existence of a backward bifurcation, and the area of backward bifurcation curve decreases as the value b_1 increases.

7 The model with fractional derivative

We consider the model with the Caputo–Fabrizio fractional derivatives

$$D_t^{\alpha_3} S(t) = (1 - p)b - \mu_1 S - f(S, I) + \gamma R,$$

$$D_t^{\alpha_3} I(t) = f(S) - (\mu_2 + \alpha)I,$$

$$D_t^{\alpha_3} R(t) = pb - (\mu_3 + \gamma)R + \alpha I,$$

$$\alpha = \alpha_0 + \frac{(\alpha_1 - \alpha_0)b_1}{I + b_1},$$

$$f(S, I) = \frac{\beta_1 SI}{a_1 + a_2 S + a_3 I}.$$

Here we have $0 < \alpha_3 < 1$ and

$$D_t^{\alpha_3} = \frac{1}{\Gamma(1 - \alpha_3)} \int_0^t f(\tau)'(t - \tau)^{-\alpha_3} \, d\tau. \tag{45}$$

We present the existence of positive solution of the system,

$$D_t^{\alpha_3} S(t) = (1 - p)b - \mu_1 S - f(S, I) + \gamma R \geq -\mu_1 S - f(S, I) \geq -\mu_1 S. \tag{46}$$

Then

$$S(t) \geq S(0) \exp\left(-\mu_1 t^{\alpha_3}\right) \quad \text{for all } t \in [0, t].$$

We can similarly show that

$$I(t) \geq I(0) \exp\left(-(\mu_2 + a_0)t^{\alpha_3}\right) \quad \text{for all } t \in [0, t].$$

$$R(t) \geq R(0) \exp\left(-(\mu_3 + \gamma)t^{\alpha_3}\right) \quad \text{for all } t \in [0, t].$$

Thus for all $t \in [0, t]$, we have that $S(t), I(t),$ and $R(t)$ are positive.

7.1 Existence and uniqueness

Here we present the condition under which the system of equations has a unique solution. To achieve this, we have

$$S(t) - S(0) = \frac{1}{\Gamma(\alpha_3)} \int_0^t f_1(S, I, R, \tau)_1(t - \tau)^{\alpha_3 - 1} \, d\tau. \tag{47}$$

$$I(t) - I(0) = \frac{1}{\Gamma(\alpha_3)} \int_0^t f_2(S, I, R, \tau)_2(t - \tau)^{\alpha_3 - 1} \, d\tau. \tag{48}$$

$$R(t) - R(0) = \frac{1}{\Gamma(\alpha_3)} \int_0^t f_3(S, I, R, \tau)_3 (t - \tau)^{\alpha_3 - 1} \, d\tau. \tag{49}$$

We will show that, for all $i = 1, 2, 3$,

(1) $|f_i(x_i, t)|^2 \leq k_i(|x_i|^2 + 1)$ and

(2) $|f_i(x_i, t) - f_i(x_i', t)|^2 \leq k_i(|x_i - x_i'|^2)$:

$$\left| f_1(S, I, R, \tau) \right|^2$$

$$= \left| (1-p)b - \mu_1 S - \frac{\beta S I}{a_1 + a_2 S + a_3 I} + \gamma R \right| \tag{50}$$

$$\leq 4\big((1-p)b\big)^2 + 4\mu_1 |S|^2 + 4\gamma^2 |R|^2 + \frac{4\beta^2 |S|^2 |I|^2}{|a_1 + a_2 S + a_3 I|^2} \tag{51}$$

$$\leq 4(1-p)^2 b^2 + 4\mu_1^2 |S|^2 + 4\gamma^2 |R|^2 + \frac{4\beta^2 \sup(|S|^2 |I|^2)}{\min |a_1 + a_2 S + a_3 I|^2} \tag{52}$$

$$\leq 4(1-p)^2 b^2 + 4\mu_1^2 |S|^2 + 4\gamma^2 \|R\|_\infty^2 + 4\mu_1^2 + \frac{4\beta^2 \|I\|_\infty^2}{M} |S|^2 \tag{53}$$

$$\leq \big(4(1-p)^2 b^2 + 4\mu_1^2 |S|^2 + 4\gamma^2 \|R\|_\infty^2\big)$$

$$\times \left(1 + \frac{4\mu_1^2 + \frac{4\beta^2 \|I\|_\infty^2}{M} |S|^2}{4(1-p)^2 b^2 + 4\mu_1^2 |S|^2 + 4\gamma^2 \|R\|_\infty^2} \right) \tag{54}$$

$$\leq \big(4(1-p)^2 b^2 + 4\mu_1^2 |S|^2 + 4\gamma^2 \|R\|_\infty^2\big)\big(1 + |S|^2\big) \tag{55}$$

$$\leq k_1\big(1 + |S|^2\big) \quad \text{if} \quad \frac{4\mu_1^2 + \frac{4\beta^2 \|I\|_\infty^2}{M}}{4(1-p)^2 b^2 + 4\gamma^2 \|R\|_\infty^2} < 1, \tag{56}$$

$$\left| f_1(S, I, R, \tau) - f(S_1, I, R, \tau) \right|^2$$

$$= \left| -\mu_1(S - S_1) - \frac{\beta(S - S_1)I}{a_1 + a_2 S + a_3 I} \right|^2 \tag{57}$$

$$\leq 2\mu_1 S - S_1|^2 + 2\beta^2 \left| \frac{I}{a_1 + a_2 S + a_3 I} \right|^2 |S - S_1|^2 \tag{58}$$

$$\leq 2\mu_1 |S - S_1|^2 + 2\beta^2 \left| \sup \frac{I}{a_1 + a_2 S + a_3 I} \right|^2 |S - S_1|^2 \tag{59}$$

$$\leq 2\mu_1 |S - S_1|^2 + 2\beta^2 M |S - S_1|^2 \leq k_2 |S - S_1|^2, \tag{60}$$

$$\left| f_2(S, I, R, \tau) \right|^2$$

$$= \left| f(S, I) - (\mu_2 + \alpha)I \right|^2 \tag{61}$$

$$\leq \sup \left| f(S) - (\mu_2 + \alpha) \right|^2 |I|^2 \leq k_3\big(1 + |I|^2\big), \tag{62}$$

where

$$k_3 = \sup \left| f(S) - (\mu_2 + \alpha) \right|^2, \tag{63}$$

$$\left| f_2(S, I, R, \tau) - f(S, I_1, R, \tau)_2 \right|^2 \leq k_3 |I - I_1|^2, \tag{64}$$

$$\left| f_3(S, I, R, \tau) \right|^2$$

$$= \left| pb - (\mu_3 + \gamma)R + \alpha I \right|^2 \tag{65}$$

$$\leq 3(pb)^2 + 3(\mu_3 + \gamma)^2|R|^2 + 3|\alpha|^2|I|^2 \tag{66}$$

$$\leq 3(pb)^2 + 3(\mu_3 + \gamma)^2|R|^2 + 3\sup|\alpha|^2|I|^2 \tag{67}$$

$$\leq 3(pb)^2 + 3(\mu_3 + \gamma)^2|R|^2 + M_1 \tag{68}$$

$$\leq 3\big((pb)^2 + M_1\big)\big(1 + \frac{(\mu_3 + \gamma)^2}{(pb)^2 + M_1}|R|^2\big) \tag{69}$$

$$\leq 3\big((pb)^2 + M_1\big)\big(1 + |R|^2\big) \quad \text{if } \frac{(\mu_3 + \gamma)^2}{(pb)^2 + M_1} < 1, \tag{70}$$

$$\big|f_3(S,I,R,\tau) - f_3(S,I,R_3,\tau)_2\big|^2 = (\mu_3 + \gamma)^2|R - R_1|^2 \leq k_4|R - R_1|^2. \tag{71}$$

Therefore, under the condition

$$\max\left(\frac{4\mu_1^2 + \frac{4\beta^2\|I\|_\infty^2}{M}}{4(1-p)^2b^2 + 4\gamma^2\|R\|_\infty^2}, \frac{(\mu_3 + \gamma)^2}{(pb)^2 + M_1}\right) < 1, \tag{72}$$

the system admits a unique solution.

7.2 Numerical solution

In this section, we present the numerical solution of the equations. We use the numerical scheme of Atangan and Toufiq [26]. To use their scheme, we have

$$D_t^\alpha S(t) = f_1(S,I,R,\tau),$$

$$D_t^\alpha I(t) = f_2(S,I,R,\tau),$$

$$D_t^\alpha R(t) = f_3(S,I,R,\tau).$$
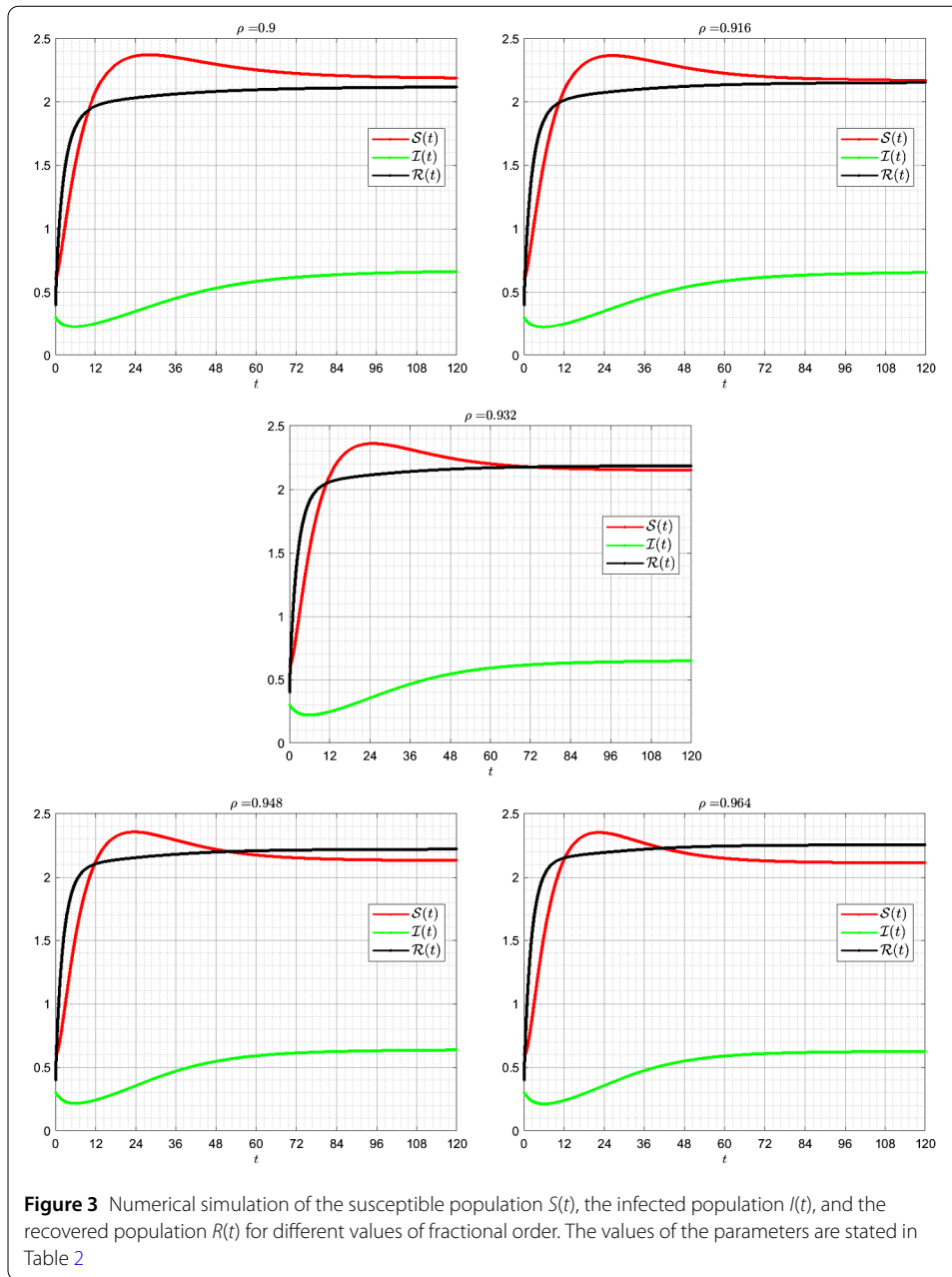
The next step is converting the above to

$$S(t) = S(0) + \frac{1}{\Gamma(\alpha_3)}\int_0^t f_1(S,I,R,\tau)(t-\tau)^{\alpha_3}\,d\tau, \tag{73}$$

$$I(t) = I(0) + \frac{1}{\Gamma(\alpha_3)}\int_0^t f_2(S,I,R,\tau)(t-\tau)^{\alpha_3}\,d\tau, \tag{74}$$

$$R(t) = R(0) + \frac{1}{\Gamma(\alpha_3)}\int_0^t f_3(S,I,R,\tau)(t-\tau)^{\alpha_3}\,d\tau. \tag{75}$$

Following their scheme, we have

$$S(t_{n+1}) = S(0) + \frac{(\triangle t)^{\alpha_3}}{\Gamma(\alpha_3 + 2)}\sum_{j=0}^n \big(f_1(S_j, I_j, R_j, \tau_j)\big)(n+1-j)^{\alpha_3}(n-j+2+\alpha_3)$$

$$- (n-j)^{\alpha_3}(n-j+1+\alpha_3))$$

$$- \big(f_1(S_{j-1}, I_{j-1}, R_{j-1}, \tau_{j-1})\big)(n+1-j)^{\alpha_3+1} - (n-j)^{\alpha_3}(n-j+1+\alpha_3)),$$

$$I(t_{n+1}) = I(0) + \frac{(\triangle t)^{\alpha_3}}{\Gamma(\alpha_3 + 2)}\sum_{j=0}^n \big(f_2(S_j, I_j, R_j, \tau_j)\big)(n+1-j)^{\alpha_3}(n-j+2+\alpha_3)$$

$$- (n-j)^{\alpha_3}(n-j+1+\alpha_3))$$

Figure 3 Numerical simulation of the susceptible population *S*(*t*), the infected population *I*(*t*), and the recovered population *R*(*t*) for different values of fractional order. The values of the parameters are stated in Table 2

$$
- \big(f_2(S_{j-1}, I_{j-1}, R_{j-1}, \tau_{j-1})\big)(n + 1 - j)^{\alpha_3 + 1}
$$

$$
- (n - j)^{\alpha_3}(n - j + 1 + \alpha_3)),
$$

$$
R(t_{n+1}) = R(0) + \frac{(\triangle t)^{\alpha_3}}{\Gamma(\alpha_3 + 2)} \sum_{j=0}^{n} \big(f_3(S_j, I_j, R_j, \tau_j)\big)(n + 1 - j)^{\alpha_3}(n - j + 2 + \alpha_3)
$$

$$
- (n - j)^{\alpha_3}(n - j + 1 + \alpha_3))
$$

$$
- \big(f_3(S_{j-1}, I_{j-1}, R_{j-1}, \tau_{j-1})\big)(n + 1 - j)^{\alpha_3 + 1} - (n - j)^{\alpha_3}(n - j + 1 + \alpha_3)).
$$

Figure 3 shows numerical simulations for different values of fractional order. We observe a slight change in the behavior of curves as the values of fractional order increase.

8 Conclusion

In this paper, we considered the SIR model with general incidence rate function and nonlinear recovery rate to model the spread of disease. The nonlinear recovery rate depends on the influence of health system.

We proved the existence, uniqueness, and boundedness of the model solution. We studied all possible steady-state solutions of the model and details of stability and also derived the reproductive number. The analysis shows that the free steady state is locally stable when the reproductive number is less than unity and unstable otherwise. The model shows the phenomenon of backward bifurcation when $R_0 < 0$ and the parameter b_1 is less than the critical value given by

$$b_1 < b_{1,\text{cr}} = \frac{\mu_1 S_0 [a_2(\mu_3 + \gamma_1)(\alpha_1 - \alpha_0)S_0 + a_1(\mu_3 + \gamma_1)(\alpha_1 - \alpha_0)]}{[\alpha_1 + \mu_2][S_0 a_3 \mu_1(\mu_3 + \gamma_1) + a_1(\alpha_1 \mu_3 + \mu_2[\gamma_1 + \mu_3])]}. \tag{76}$$

When the parameter b_1 is sufficiently greater that the critical value $b_{1,\text{cr}}$, the disease infection decreases because the number of hospital beds increases. Therefore, to treat the disease in a community, the hospital resources must be improved.

Finally, we applied the theory of fractional derivatives to the model for different values of fractional orders. We used the numerical technique of Atangan and Toufiq, which is very accurate for solving fractional differential equations.

Publisher's Note
Springer Nature remains neutral with regard to jurisdictional claims in published maps and institutional affiliations.

References
1. Ndaïrow, F., Area, I., Nieto, J.J., Torres, D.F.M.: Mathematical modeling of COVID-19 transmission dynamics with a case study of Wuhan. Chaos Solitons Fractals **135**, 109846 (2020)
2. Mandal, M., Jana, S., Nandi, S.K., Khatua, A., Adak, S., Kar, T.K.: A model based study on the dynamics of COVID-19: prediction and control. Chaos Solitons Fractals **136**, 109889 (2020)
3. Lin, Q., Zhao, S., Gao, D., Lou, Y., Yang, S., Musa, S.S., Wang, M.H., Cai, Y., Wang, W., Yang, L., He, D.: A conceptual model for the coronavirus disease 2019 (COVID-19) outbreak in Wuhan, China with individual reaction and governmental action. Int. J. Infect. Dis. **93**, 211–216 (2020)
4. Wells, C.R., Sah, P., Moghadas, S.M., Pandey, A., Shoukat, A., Wang, Y., Wang, Z., Meyers, L.A., Singer, B.H., Galvani, A.P.: Impact of international travel and border control measures on the global spread of the novel 2019 coronavirus outbreak. Proc. Natl. Acad. Sci. USA **117**, 7504–7509 (2020)
5. Gostic, K., Gomez, A.C.R., Mummah, R.O., Kucharski, A.J., Lloyd-Smith, J.O.: Estimated effectiveness of symptom and risk screening to prevent the spread of COVID-19. eLife **9**, e55570 (2020)
6. Chen, Y.-C., Lu, P.-E., Chang, C.-S., Liu, T.-H.: A time-dependent SIR model for Covid-19 with undetectable infected persons (2020). arXiv:2003.00122
7. Anand, N., Sabarinath, A., Geetha, S., et al.: Predicting the spread of COVID-19 using SIR model augmented to incorporate quarantine and testing. Trans Indian Natl. Acad. Eng. **5**, 141–148 (2020)

8. Nguemdjo, U., Meno, F., Dongfack, A., Ventelou, B.: Simulating the progression of the COVID-19 disease in Cameroon using SIR models. PLoS ONE **15**, 8 (2020)
9. Greenhalgh, D., Khan, Q., Lewis, F.: Hopf bifurcation in two SIRS density dependent epidemic models. Math. Comput. Model. **39**, 11 (2004)
10. Tang, Y., Huang, Y., Ruan, S., Zhang, W.: Coexistence of limit cycles and homoclinic loops in a SIRS model with a nonlinear incidence rate. SIAM J. Appl. Math. **69**, 2 (2008)
11. Yakui, X., Tiantian, L.: Stability and Hopf bifurcation for a delayed SIR epidemic model with logistic growth. Abstr. Appl. Anal. **2013**, Article ID 916130 (2013)
12. Tailei, Z., Junli, L., Zhidong, T.: Stability of Hopf bifurcation of a delayed SIRS epidemic model with stage structure. Nonlinear Anal., Real World Appl. **11**, 293–306 (2010)
13. Sonal, J.: Numerical analysis for the fractional diffusion and fractional Buckmaster's equation by two step Adam–Bashforth method. Eur. Phys. J. Plus **133**, 19 (2018)
14. Abdon, A., Sonal, J.: A new numerical approximation of the fractal ordinary differential equation. Eur. Phys. J. Plus **133**, 37 (2018)
15. Sania, Q., Mokhi, C., Asif Ali, S.: Analysis of series RL and RC circuits with time-invariant source using truncated M, atangana beta and conformable derivatives. J. Ocean Eng. Sci. (2020)
16. Zizhen, Z., Sonal, J.: Mathematical model of Ebola and Covid 19 with fractional differential operators: non-Markovian process and class for virus pathogen in the environment. Chaos Solitons Fractals **140**, 110175 (2020)
17. Ernestine, A., Abdon, A.: Facemasks simple but powerful weapons to protect against COVID-19 spread: can they have sides effects?. Results Phys. **19**, 103425 (2020)
18. Rao, F., Mandal, P.S., Kang, Y.: Complicated endemics of an SIRS model with a generalized incidence under preventive vaccination and treatment controls. Appl. Math. Model. **67**, 38–61 (2019)
19. Shan, C., Zhu, H.: Bifurcations and complex dynamics of an SIR model with the impact of the number of hospital beds. J. Differ. Equ. **257**, 1662–1688 (2014)
20. Cai, Y., Kang, Y., Banerjee, M., Wang, W.: A stochastic SIRS epidemic model with infectious force under intervention strategies. J. Differ. Equ. **259**, 7463–7502 (2015)
21. Lahrouz, A., Omari, L., Kiouach, D., Belmaâti, A.: Complete global stability for an SIRS epidemic model with generalized non-linear incidence and vaccination. Appl. Math. Comput. **218**, 6519–6525 (2012)
22. Xiao, D., Ruan, S.: Global analysis of an epidemic model with nonmonotone incidence rate. Math. Biosci. **208**, 419–429 (2007)
23. Abdelrazec, A., Belair, J., Shan, C., Zhu, H.: Modeling the spread and control of Dengue with limited public health resources. Math. Biosci. **271**, 136–145 (2016)
24. Driessche, P., Watmough, J.: Reproduction numbers and sub-threshold endemic equilibria for compartmental models of disease transmission. Math. Biosci. **180**, 29–48 (2002)
25. Castillo-Chavez, C., Song, B.: Dynamical models of tuberculosis and their applications. Math. Biosci. Eng. **1**, 361–404 (2004)
26. Mekkaoui, T., Abdon, A.: New numerical approximation of fractional derivative with non-local and non-singular kernel: application to chaotic models. Eur. Phys. J. Plus **132**, 444 (2017)